THE JOURNAL OF BIOLOGICAL CHEMISTRY
Vol. 277, No. 43, Issue of October 25, pp. 40575–40582, 2002

Printed in U.S.A.

The N Terminus of Mannose 6-Phosphate/Insulin-like Growth Factor 2 Receptor in Regulation of Fibrinolysis and Cell Migration*

Received for publication, August 5, 2002
Published, JBC Papers in Press, August 19, 2002, DOI 10.1074/jbc.M207979200

Vladimír Leksa‡, Samuel Godár‡, Marek Cebecauer§, Ivan Hilgert§, Johannes Breuss¶, Ulrich H. Weidle‖, Václav Horejsí§, Bernd R. Binder¶, and Hannes Stockinger‡**

From the ‡Institute of Immunology, Vienna International Research Cooperation Center at Novartis Forschungs-institut, University of Vienna, Vienna A-1235, Austria, the §Institute of Molecular Genetics, Academy of Sciences of the Czech Republic, Prague 4-14220, Czech Republic, the ¶Department of Vascular Biology and Thrombosis Research, University of Vienna, Vienna A-1090, Austria, and ‖Roche Diagnostics, Division Pharma, Penzberg D-82372, Germany

Leukocyte migration to sites of inflammation is a multistep process involving transient adhesion to the endothelium followed by cell surface-controlled proteolysis for transmigration through the vessel wall and chemotactic movement within tissues. One of the key players in this machinery appears to be the urokinase-type plasminogen activator (uPA)/uPA receptor system. The role of uPA and its receptor (CD87) in plasminogen (Plg) activation, cell adhesion, and chemotaxis is well established; however, less is known of how these activities are regulated. Here we provide evidence that the mannose 6-phosphate/insulin-like growth factor 2 receptor (CD222) controls CD87-mediated functions. Expression of human CD222 in CD222−/− mouse fibroblasts downregulated Plg activation, cell adhesion, and chemotaxis induced by the uPA/CD87 system. In addition, we demonstrate that the N-terminal region of CD222, which is similar to the Plg-binding site of streptokinase, plays a crucial role in binding of CD87 and Plg. A peptide derived from this region in CD222 is able to disrupt the physical interaction of CD222 with CD87 and, furthermore, mimics the inhibitory effects of CD222 on CD87 functions. Taken together, our results indicate a novel role for CD222 in regulation of fibrinolysis, cell adhesion, and migration.

The migration of leukocytes toward the site of inflammation is a complex process in which several mechanisms are harnessed. First, leukocyte adhesion to the endothelium is mediated by a variety of receptors expressed on both leukocytes and endothelial cells. Second, cell surface-mediated proteolysis facilitates leukocyte transmigration across the vessel walls by degrading extracellular matrix proteins and basement membrane. Third, chemoattractants produced at the site of injury promote leukocyte locomotion within target tissues (1, 2). This machinery is not restricted to leukocytes but used by all cells that migrate including tumor cells.

One of the key players in this cell migration event seems to be the urokinase-type plasminogen activator (uPA)[1] receptor (CD87). CD87 is a highly glycosylated 50–65-kDa protein linked to the plasma membrane by glycosylphosphatidylinositol (GPI) (3, 4). CD87 is expressed on a multitude of cells including monocytes, neutrophils, activated T cells, endothelial cells, and tumor cells. It mediates generation of cell-surface proteolytic activity by binding pro-urokinase (pro-uPA). Receptor-bound pro-uPA can be activated to uPA, which in turn activates cell-bound plasminogen (Plg) to plasmin, a serine protease with broad substrate specificity (5). This conveys to cells a proteolytic potential required for remodeling of pericellular space during migration. Independently of its function in the fibrinolytic (Plg/plasmin) system, CD87 was shown to have further roles in cell migration (6, 7). It was demonstrated that the binding of uPA to CD87 induced adhesion of myeloid cells to the matrix protein vitronectin (8, 9). In addition, uPA promoted the chemotactic movement of different cell types (10–13).

It has been suggested that the interaction of CD87 with integrins and caveolin participates in regulation of cell adhesion and in focusing of pericellular proteolysis to specific extracellular sites (14–17). In addition, specific inhibitors (plasminogen activator inhibitor type 1 (PAI-1) and type 2 (PAI-2)) control the activity of uPA. Once formed, the complex of PAI-1·uPA·CD87 is immediately internalized by the low density lipoprotein receptor-related protein/α_2-macroglobulin receptor (CD91). This leads to lysosomal degradation of uPA and subsequent recycling of disengaged CD87 back to the cell surface (18, 19).

However, recent studies indicate that there is also an additional mechanism able to internalize CD87 independently of the CD91 pathway (20). This mechanism may be mediated by the cation-independent mannose 6-phosphate/IGF2 receptor, recently assigned as CD222 (21). CD222 is a ubiquitously expressed 250-kDa type I transmembrane protein. The majority of CD222 molecules (~90–95%) are located intracellularly; only 5–10% are present on the cell membrane. CD222 is a multifunctional receptor binding a multitude of ligands. It transports newly synthesized lysosomal enzymes, modified by mannose 6-phosphate residues (M6-P), from the Golgi apparatus to lysosomes; however, it also binds and internalizes exogenous M6-P-containing ligands. Furthermore, it is crucial for the internalization and degradation of IGF2 and thereby controls cell growth (22–24). CD222 binds also CD87 and, notably,

* This work was supported by the Austrian Science Fund. Part of the work was performed within the Biomolecular Therapeutics Research Consortium. The costs of publication of this article were defrayed in part by the payment of page charges. This article must therefore be hereby marked "*advertisement*" in accordance with 18 U.S.C. Section 1734 solely to indicate this fact.

** To whom correspondence should be addressed: Inst. of Immunology, Vienna International Research Cooperation Center at NFI, University of Vienna, Vienna A-1235, Austria. Tel.: 43-1-4277-64999; Fax: 43-1-4277-64998; E-mail: hannes.stockinger@univie.ac.at.

[1] The abbreviations used are: uPA, urokinase-type plasminogen activator; BB, binding buffer; BSA, bovine serum albumin; GPI, glycosylphosphatidylinositol; IGF2, insulin-like growth factor 2; LB, lysis buffer; M6-P, mannose 6-phosphate; mAb, monoclonal antibody; PAI, plasminogen activator inhibitor; PBMC, peripheral blood mononuclear cell; PBS, phosphate-buffered saline; pepA, peptide A; pepB, peptide B; pepB*scr*, scrambled peptide B; pepC, peptide C; Plg, plasminogen; TA, tranexamic acid.

Plg (25, 26). Thus, CD222 is a receptor for two critical components of the fibrinolytic system. This tempted us to speculate that CD222 is involved in the regulation of fibrinolysis.

In the present study we show that, in fact, CD222 has a general impact on CD87 functions. By employing CD222-deficient mouse fibroblasts expressing human CD222 and human CD87, we demonstrate that CD222 regulates CD87-dependent Plg activation, cell adhesion, and chemotaxis. Furthermore, we identified an amino acid stretch in CD222 to be involved in binding and regulation of CD87.

MATERIALS AND METHODS

Antibodies and Reagents—The mouse CD87 monoclonal antibodies (mAbs) H2 and C8 were obtained as a result of immunization with recombinant soluble human CD87 (amino acids 1–277), which was constructed and purified from supernatants of stably transfected Chinese hamster ovary cells as described (27). The mouse mAbs MEM-238 and MEM-240 against CD222 were obtained in our laboratories by standard techniques from mice immunized with recombinant vaccinia virus containing CD222 (21). The anti-pTag mAb H902-producing hybridoma cell line is reagent 521 from the National Institutes of Health AIDS Research and Reference Program. Peptide B (pepB, AVDTKNNVLYKINIAGSV), a scrambled version of pepB (pepB*scr*, DILVNGAKVATKIVNYNS), and peptide C (pepC, HDLKTRTYHSVGDSVLRS) were synthesized by Genosphere Biotechnologies (Paris, France); peptide A (pepA, QYLFSWYT) was synthesized by Pichem (Graz, Austria). Vitronectin, pro-uPA, uPA, Glu-Plg, and PAI-1, all of human origin, were products of Technoclone (Vienna, Austria). Human fibronectin, rat collagen-1, and mouse laminin were from Upstate Biotechnology, Inc. (Lake Placid, NY). Anti-mouse alkaline-phosphatase conjugate, Polybrene, all protease inhibitors, crystal violet, Triton X-100, and tranexamic acid (TA) were from Sigma. Nonidet P-40 was obtained from Pierce and plasmin substrate S-2251 from Chromogenix (Milano, Italy). BSA was a product of Behring (Marburg, Germany). All enzymes used in PCR and cloning techniques were from Roche Diagnostics (Penzberg, Germany). Primers and linkers were produced by Vienna Biocenter (Vienna, Austria).

Cell Cultures—The NIH3T3 cell line and the CD222-negative mouse fibroblasts kindly provided by Dr. E. Wagner (28) were cultured in RPMI 1640 medium supplemented with penicillin, streptomycin, glutamine, and 10% fetal calf serum. The ecotropic packaging cell line Phoenix, generously provided by Dr. G. P. Nolan (29), was cultured in Dulbecco's modified Eagle's medium under standard conditions. Human peripheral blood mononuclear cells (PBMCs) were isolated from blood of healthy individuals by density gradient centrifugation in Ficoll-Hypaque. Monocytes were separated by 1-h adhesion to plastic.

Generation of the Retroviral Plasmid Constructs—The 8-kb fragment of the full-length human CD222 cDNA fused to the pTag DNA (26) was cleaved from the CDM8 vector with *Xba*I, blunt-ended, and cloned into the *Eco*RI sites of the retroviral vector BMN-Z (30) via *Mun*I linkers. The resultant construct CD222-pTag/BMN-Z coding for the full-length receptor (Δ0) was then used for the generation of six truncated receptor constructs; the partial cleavage of CD222-pTag/BMN-Z with *Hin*dIII and subsequent ligation resulted in the constructs with deletions 573–3791, 573–2090, and 2090–3791 in the CD222 cDNA, coding for the proteins truncated of amino acids 191–1263 (Δ2–9), 191–696 (Δ2–5), and 696–1263 (Δ6–9), respectively. The cleavage of the CD222-pTag/BMN-Z with *Aat*II and subsequent ligation resulted in the construct with deletion 3808–6161, coding for the protein truncated of amino acids 1269–2053 (Δ9–14). A 670-bp fragment was amplified by PCR from CD222-pTag/BMN-Z using the primers 5′-TGTCAGAATTCAGCCAGGCAGTCGGCGCGG-3′ containing an *Eco*RI site and 5′-CCGCCTCGAGTTTTCCTATTGTAACAAATGCTC-3′ containing an *Xho*I site. The fragment was cleaved with *Eco*RI and *Xho*I and ligated between the *Eco*RI (position 329 in the CD222 cDNA) and *Xho*I site (position 91 in the pTag DNA) of CD222-pTag/BMN-Z. This resulted in the construct with the deletion 330–6902, coding for the protein truncated of amino acids 110–2300 (Δ0.5–15). Arg^{2301} was replaced by Phe in this truncated form. Furthermore, an 800-bp fragment was amplified by PCR from CD222-pTag/BMN-Z using the primers 5′-ATATGAGATCTTATATGGGGCACCCCCGCC-3′ containing a *Bgl*II site and 5′-TCGGGGAATTCGGCGGCCTGGGCCTGC-3′ containing an *Eco*RI site. The fragment was cleaved with *Bgl*II and *Eco*RI and ligated into the CD222-pTag construct between the *Bgl*II (position 1930 in BMN-Z) and the *Eco*RI site (position 329 in the CD222 cDNA). This resulted in the construct with the deletion 131–329, coding for the protein truncated of the amino acids 44–109 (Δ0.5). Pro^{44} was replaced by Glu. To prepare a retroviral plasmid containing the non-tagged full-length CD222 cDNA, the *Nsi*I and *Sal*I fragment of CD222-pTag in pBMN-Z was replaced by the 6.6-kb *NsiI*/*Sal*I fragment of CD222 in the pGEM vector (American Type Culture Collection, Rockville, MD).

The 1.4-kb fragment with the full-length human CD87 DNA was cleaved from the pKCR vector with *Nru*I and *Sac*I, blunt-ended, and cloned into the *Eco*RI sites of the retroviral vector BMN-Z via the *Mun*I linkers. The construct CD147-pTag/BMN-Z was a gift from Günther Staffler.

Generation of Stably Transduced Cells—All transfection and transduction procedures were as described (Refs. 29 and 31; www-leland.stanford.edu/group/Nolan). Briefly, the retroviral plasmids were used for transient transfection of the ecotropic packaging cell line Phoenix by the Superfect Transfection method (Qiagen, Hilden, Germany). Three days after transfection, the supernatants containing viral particles were mixed with Polybrene (4 μg/ml) and the mixtures were used to transduce target cells. CD222-negative mouse fibroblasts were transduced with human CD222, CD87, and both receptors; NIH3T3 cells were transduced with the pTag-tagged full-length and truncated forms of CD222. The expression of the recombinant proteins was verified by fluorescence-activated cell sorting staining with specific mAbs; positive cells were selected by limiting dilution for further study.

Flow Cytometry—Cells were detached, washed, and incubated with PBS containing 1% BSA and the primary mAbs for 20 min on ice. After washing, cells were incubated with fluorescein isothiocyanate-conjugated sheep $F(ab')_2$ anti-mouse IgG+IgM (H+L) antibodies (An der Grub, Kaumberg, Austria) for 20 min on ice, again washed, and analyzed with a flow cytometer (FACScan, Becton Dickinson, Heidelberg, Germany).

Purification of Receptor Proteins—Transductants (5×10^7) were lysed for 30 min on ice in lysis buffer (LB; 20 mM Tris-HCl, 140 mM NaCl, pH 8.2) containing 1% Nonidet P-40 as a detergent and a mixture of protease inhibitors (5 mM iodoacetamide, 10 μg/ml aprotinin, 10 μg/ml leupeptin, 1 mM phenylmethylsulfonyl fluoride, 0.1 mM quercetin, 0.1 mM *N*-tosyl-L-phenylalanine chloromethyl ketone, 0.1 mM N^{α}-*p*-tosyl-L-lysine chloromethyl ketone, 0.1 mM *N*-CBZ-L-phenylalanine chloromethyl ketone, 1 mM pepstatin A). Lysates were centrifuged for 5 min at 10,000 × *g* at 4 °C, and the supernatants were subjected to affinity chromatography using anti-pTag mAb H902 coupled to Sepharose. The columns were washed with LB, and purified receptor proteins were eluted from the column with elution buffer (20 mM Tris-HCl, 140 mM NaCl, pH 11.7). The eluted fractions were adjusted to pH 7.5 using HCl.

In Vitro Binding Assay—Ten μg/ml amounts of various molecules were coated on a 96-well Falcon plate in PBS (pH 8.7) for 2 h at 37 °C. The wells were blocked with 1% BSA in PBS for 1 h at room temperature and washed two times with binding buffer (BB; 20 mM Tris-HCl, 140 mM NaCl, pH 7.5). Wells were then incubated 4 h on ice with BB supplemented with 5 μg/ml purified receptors in the absence or presence of additional molecules and washed two times with ice-cold BB. Bound material was separated by SDS-PAGE followed by transfer to Immobilon polyvinylidene difluoride membranes (Millipore Co., Bedford, MA). Membranes were blocked by using 4% nonfat milk and immunostained with specific mAbs. For visualization of proteins, the ECL system and the Lumi-Imager were used (Roche Diagnostics, Mannheim, Germany).

Immunoprecipitation—All procedures were done as described (14). Briefly, cells (5×10^7 mouse fibroblast transductants or purified human monocytes) were lysed in LB containing 1% Nonidet P-40 and the mixture of protease inhibitors (see above). Cell lysates were subjected to immunoprecipitation using specific mAbs coated on a 96-well Falcon plastic plate via goat anti-mouse Ig (H+L) antibodies (Southern Biotechnology Associates, Inc., Birmingham, AL). After 3 h at 4 °C the immunoprecipitates were washed and analyzed by SDS-PAGE and immunoblotting.

Plasminogen Activation Assay—We slightly modified a previously described method (32). After harvesting by trypsinization, mouse fibroblasts were seeded into a 96-well plate (Nunc, Roskilde, Denmark) at a density of 2×10^3 or 2×10^4 cells/well and cultured in RPMI 1640 medium containing 10% fetal calf serum to subconfluence or confluence, respectively. Monocytes were separated from human PBMCs by 1-h adhesion to a 96-well plate (1×10^6/well). Cell monolayers were washed with serum-free medium, incubated with 3 nM pro-uPA at 37 °C for 20 min. After washing twice, Plg (50 nM) and the chromogenic plasmin substrate S-2251 (0.8 mM) were added. Cells were incubated at 37 °C, and after different time intervals the absorbance change at 405 nm was

monitored by using an enzyme-linked immunosorbent assay reader (Anthos Labtec Instruments, Salzburg, Austria).

Adhesion Assay—Cells were harvested, washed, and resuspended in serum-free medium. Various matrix proteins as indicated were coated on a 96-well plate (Nunc) in RPMI 1640 medium for 2 h at 37 °C. Wells were blocked by using 1% BSA, washed and then incubated either with mouse fibroblasts (1×10^4/well) or with human PBMCs (1×10^6/well) in the presence or absence of 10 nM uPA. After 40-min incubation at 37 °C, wells were washed gently by immersion in a plastic tray containing RPMI 1640 medium. Adhered cells were fixed by methanol and stained by crystal violet. After intense washings, cells were solubilized in 0.5% Triton X-100 and the number of cells was determined by measuring the absorbance at 595 nm using an enzyme-linked immunosorbent assay reader.

Chemotaxis Assay—Chemotaxis analysis was performed in a 24-well plate using tissue culture polycarbonate filter inserts (10-mm diameter, 8-μm pore size, Nunc) coated with vitronectin (10 μg/ml) and blocked with BSA. Mouse fibroblasts (5×10^4) or human PBMCs (1×10^6) prepared as for the adhesion assay were resuspended in 300 μl of serum-free medium and loaded into the upper chamber of an insert. Ten nM uPA in 300 μl of serum-free medium was added into the lower chamber. After 4-h incubation at 37 °C, the filters were removed, the upper surface of the membrane was scraped free of cells, and the number of cells that had migrated to the lower surface was measured by crystal violet as described before.

Statistical Analysis—The experiments shown in Figs. 2, 3, 4, 9, and 10 were performed at least three times in duplicate. A two-sided Student's t test was used for the statistical evaluation, and p values <0.05 were considered significant.

RESULTS

Generation of Cells Expressing Human CD222, Human CD87, or Both Receptors—Our previous study demonstrated physical interaction of CD222 with CD87 on the surface of monocytes (26). However, a cell system with CD222-negative background was required to investigate the functional consequences of this interaction. Mouse fibroblasts derived from CD222-deficient embryos (−/−) appeared to be suitable for that purpose. By using a retroviral system, we engineered these cells to express human CD222 ($CD222^+$), human CD87 ($CD87^+$) or both receptors ($CD222^+/CD87^+$) (see "Materials and Methods"). Cell surface expression on the transductants was evaluated by immunofluorescence analysis and flow cytometry using CD222 and CD87 mAbs. Fig. 1 shows a low CD222 surface expression that is similar to the expression of native CD222 on human cells (CD222 is mainly expressed intracellularly with only 5–10% on the cell surface (Ref. 22)). To test whether CD87 and CD222 also interact physically in the transductants, we solubilized $CD222^+/CD87^+$ cells using Nonidet P-40 as a detergent and subjected the lysate to immunoprecipitation followed by immunoblotting analysis. Immunoprecipitates obtained by the CD87 mAb H2 (Fig. 1, *inset*) or CD222 mAb MEM-240 (data not shown) contained both CD87 and CD222 as demonstrated by blotting with the CD87 mAb C8 or the CD222 mixture (mix of CD222 mAbs MEM-238 and MEM-240). This indicated that, not only in monocytes but also in the mouse fibroblast transductants, CD222 and CD87 were physically associated. Thus, the cell system generated by us was considered to be appropriate to analyze the functional consequence of this interaction.

CD222 Regulates CD87-dependent Functions—We analyzed the effect of the CD222-CD87 interaction on CD87-mediated Plg activation, cell adhesion, and chemotaxis. First, the ability of the engineered cells to activate Plg was tested. Cells were preincubated with human pro-uPA, washed, and then incubated with Plg together with the chromogenic plasmin substrate S-2251. As can be seen in Fig. 2, $CD87^+$ cells activated Plg at a rate ~4-fold higher than did −/− cells. In contrast, when CD222 was co-expressed with CD87 in $CD222^+/CD87^+$ co-transductants, Plg activation was repressed. Furthermore,

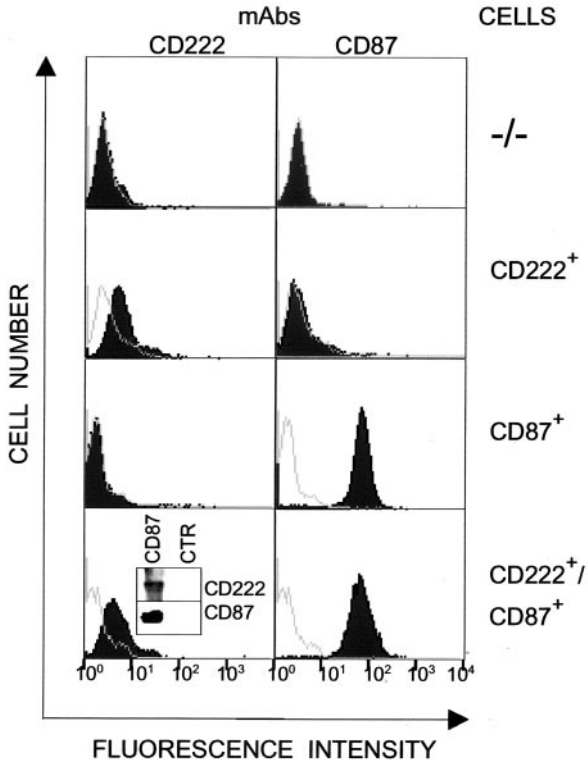

FIG. 1. **Characterization of $CD222^+/CD87^+$ mouse fibroblast transductants.** A retroviral system was used for gene transfer and expression of human CD222 ($CD222^+$), CD87 ($CD87^+$), and both receptors ($CD222^+/CD87^+$) in CD222-negative mouse fibroblasts (−/−). Cell surface expression of CD222 and CD87 was verified on subconfluent cells by immunofluorescence analysis and flow cytometry using a mixture of CD222 mAbs (MEM-238 and MEM-240) and CD87 mAb C8. The *inset* shows immunoblotting of immunoprecipitates obtained from the double positive transductant with CD87 mAb H2 and IgG control mAb H902 (*CTR*). For blotting either the CD222 mAb mix consisting of MEM-238 and MEM-240 or the CD87 mAb C8 was used.

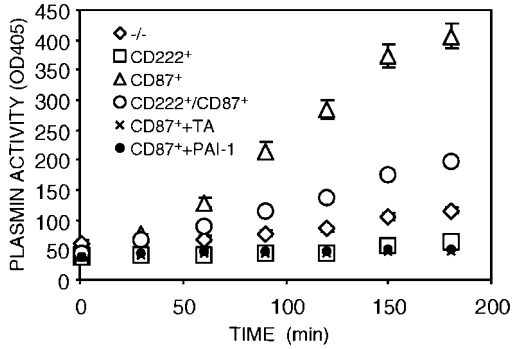

FIG. 2. **Plg activation assay.** Cells (−/−, $CD87^+$, $CD222^+$, $CD222^+/CD87^+$ mouse fibroblasts) were seeded into a 96-well plate (2×10^3 cells/well) and cultured for 24 h to subconfluence. Cell monolayers were pre-incubated for 20 min at 37 °C with serum-free medium containing 3 nM pro-uPA, washed, and then incubated with Plg (50 nM) and the chromogenic plasmin-specific substrate S-2251 (0.8 mM). Plasmin activity was detected at different time intervals by measuring the absorbance at 405 nm. Some experiments were performed in the presence of 5 mM TA or 10 units/ml PAI-1 as indicated (data obtained with $CD87^+$ cells are shown). Experiments were repeated three times in duplicate.

we found that the responses of the $CD222^+/CD87^+$ co-transductants, but not those of the $CD87^+$ single transductants, were density-dependent. Confluent $CD222^+/CD87^+$ cells displayed ~80% of the Plg activation rate of $CD87^+$ cells, whereas subconfluent $CD222^+/CD87^+$ cells showed only ~50% (Fig. 2 and data not shown). When we compared expression of CD87 and CD222 on the surface of sparse *versus* dense $CD222^+/$

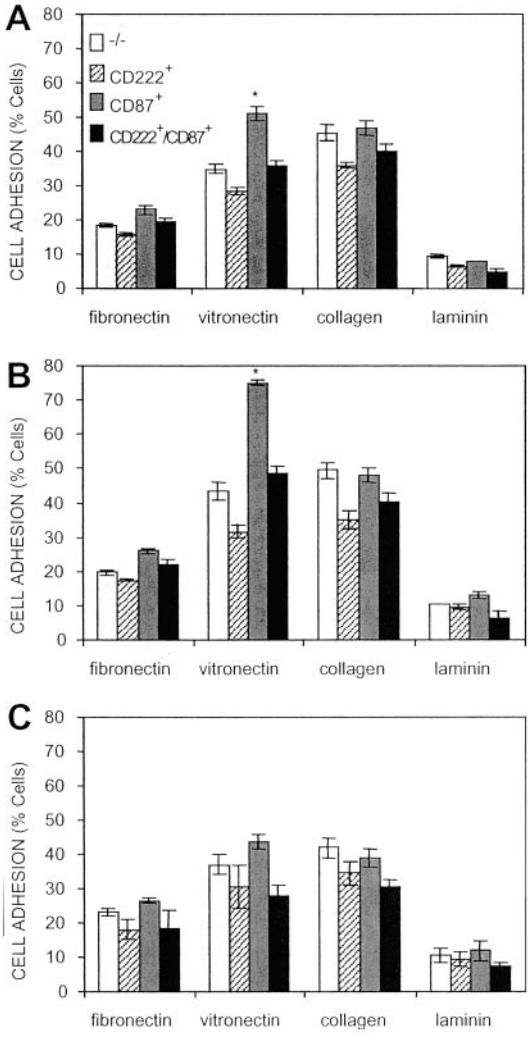

FIG. 3. **Cell adhesion assay.** Cells (−/−, CD87$^+$, CD222$^+$, CD222$^+$/CD87$^+$ mouse fibroblasts) were harvested, washed with serum-free medium, and seeded into a 96-well plate pre-coated with the indicated matrix proteins. Cells were incubated at 37 °C in medium containing no additional molecule (*A*), 10 nM uPA (*B*), or 10 nM uPA plus 10 units/ml PAI-1 (*C*). After 40 min, wells were washed, and attached cells were fixed and stained with crystal violet. The cell number was determined by measuring the absorbance at 595 nm, and cell adhesion was expressed as percentage of the total amount of cells added to the wells. Experiments were repeated three times in duplicate; the mean values ± S.D. (*, $p < 0.05$) are shown.

CD87$^+$ cells by fluorescence-activated cell sorting analysis, we saw an almost 3-fold higher surface expression of CD222 on subconfluent cells (mean fluorescence intensity 11 ± 3 *versus* 4 ± 2, $n = 3$); CD87 expression remained unchanged. This pattern was also confirmed by biochemical analysis comparing surface biotinylated *versus* total CD222 (data not shown). A similar density-dependent expression of CD222 was observed with hepatocytes (33). Thus, surface expression of endogenous CD222 appears to correlate inversely with the function of CD87. Together with the more pronounced uPA-induced responses of CD87$^+$ single transductants, this finding suggests that CD222-free forms of CD87 are responsible for the observed functional effects in our experiments. The Plg activation of the CD87$^+$ single transductant was abolished in the presence of the lysine analogue TA, an inhibitor of Plg binding to the cell surface, indicating that cell-bound Plg was required for activation (Fig. 2). Moreover, the uPA inhibitor PAI-1 also inhibited Plg activation of the CD87$^+$ cells demonstrating the uPA dependence of this process.

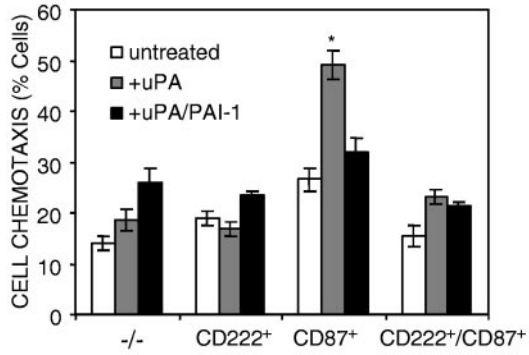

FIG. 4. **Cell chemotaxis assay.** Chemotaxis analysis was performed in a 24-well plate using tissue culture polycarbonate filter inserts. The lower sides of the insert membranes were precoated with vitronectin and blocked with BSA. Cells (−/−, CD87$^+$, CD222$^+$, CD222$^+$/CD87$^+$ mouse fibroblasts) were harvested, washed, resuspended in serum-free medium, and added to the top chamber. Medium with 10 nM uPA, uPA plus PAI-1 (10 nM plus 10 unit/ml), or no supplement was added to the bottom chamber. After 4-h incubation at 37 °C the filters were washed, the upper sides of the membranes were scraped free of cells, and the cells adhered to the lower sides were fixed and stained with crystal violet. The cell number was determined by reading the absorbance at 595 nm. Migration of cells onto the lower surface of the membrane was expressed as percentage of the total cell number seeded. Experiments were repeated six times in duplicate; the mean values ± S.D. (*, $p < 0.05$) are shown.

Second, we tested the adhesive capacity of the individual transductants. Cells were incubated in wells precoated with various matrix proteins in the absence or presence of human uPA. After washing, the number of cells that remained adhered was evaluated (Fig. 3). CD222-negative cells (−/−) adhered to collagen reproducibly stronger than to vitronectin (45 ± 3% or 35 ± 2% adherent cells, respectively). Adhesion to fibronectin was weaker (19 ± 1%), and adhesion to laminin was low (8 ± 1%). In comparison, CD87$^+$ cells manifested stronger adhesion to vitronectin (52 ± 2%, Fig. 3*A*) and this effect was significantly enhanced by uPA (74 ± 2% of adherent cells, compare Fig. 3, *A* and *B*). When CD222 was co-expressed with CD87 (CD222$^+$/CD87$^+$ cells), this CD87-mediated adhesion to vitronectin was not observed both in the uPA-treated and non-treated cells. In contrast to the adhesion to vitronectin, expression of CD87 and co-expression with CD222 had minimal or no effect on the adhesiveness of the transductants to fibronectin, collagen, and laminin. The uPA inhibitor PAI-1 blunted the CD87/uPA-induced adhesion to vitronectin demonstrating the specificity of the effect (Fig. 3*C*).

Third, we evaluated the contribution of CD222 to CD87/uPA-induced chemotaxis using modified Boyden chambers coated with vitronectin (Fig. 4). The basal migration of −/− cells was low (14 ± 1%). However, when CD87 was expressed, ~2 times more cells migrated (28 ± 2%). When uPA was added to the lower compartment of the chamber, CD87$^+$ cells increased significantly the migratory response (50 ± 3% of cells); this effect was abrogated by PAI-1. In contrast, cells co-expressing CD87 plus CD222 did not show a significantly different migration behavior in comparison to −/− cells both in the presence or absence of uPA. This result indicates a negative modulatory effect of CD222 on CD87-mediated cell migration.

The N-terminal Region of CD222 Is Critical for Binding of CD87 and Plg—To gain insight into how CD222 interacts with CD87 and Plg, we mapped the binding sites within CD222. We generated several truncated forms of CD222 lacking different regions of the extracellular part of CD222. A peptide sequence tag (termed pTag) was fused to the full-length receptor and all truncated forms for convenient purification and detection of the recombinant CD222 proteins by using the anti-pTag mAb H902

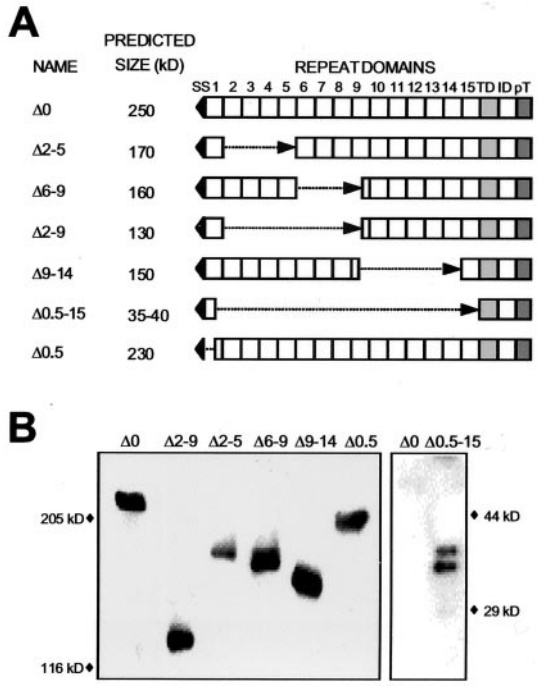

FIG. 5. **Generation of truncated forms of CD222.** *A*, full-length CD222 consists of the signal sequence at the N terminus (*SS*), 15 extracellular repeat domains (*1–15*), one transmembrane domain (*TD*), and the intracellular domain (*ID*). Designations of the constructs correspond to the deleted extracellular repeat domains as indicated. The short peptide pTag (*pT*) containing an epitope recognized by the specific mAb H902 was fused to the C termini of all constructs. Molecular weights of the recombinant CD222 proteins were predicted according to their amino acid contents. *B*, lysates prepared from NIH3T3 cells stably expressing the recombinant CD222 proteins were analyzed by SDS-PAGE followed by immunoblotting analysis using anti-pTag mAb H902. Samples were separated on either 4% (*left panel*) or 12% (*right panel*) polyacrylamide gels. Molecular weight standards are shown along the panel borders.

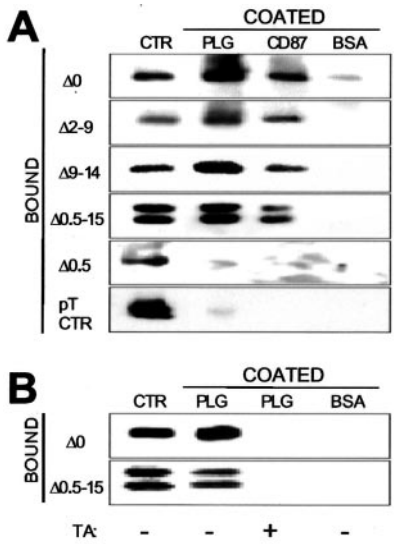

FIG. 6. **Mapping of the binding sites for Plg and CD87 within CD222.** *A*, wells of a Falcon plate were coated with 10 μg/ml Plg or soluble CD87 and blocked with BSA. After washing, wells were incubated with binding buffers containing the purified pTag-tagged full-length (*Δ0*) and truncated forms of CD222 (*Δ2–9*, *Δ9–14*, *Δ0.5–15*, *Δ0.5*) or control pTag-tagged protein (*pT CTR*, CD147-pTag). After 3-h incubation at 4 °C, wells were washed and bound material was analyzed by SDS-PAGE on a 12% (*Δ0.5–15*, *pT CTR*) or a 4% gel followed by immunoblotting using the anti-pTag mAb H902. *B*, binding analysis of Δ0 and Δ0.5–15 was performed in the absence (−) or presence (+) of 5 mM TA. Respective samples of the binding solutions were applied onto the gels as positive controls (*CTR*).

(34) (see "Materials and Methods" and Fig. 5*A* for terminology). As analyzed by SDS-PAGE, the molecular weights of the truncated receptors were in agreement to those predicted by their amino acid compositions (Fig. 5*B*). To analyze direct binding, the purified pTag-tagged full-length and truncated receptor proteins were incubated with immobilized soluble recombinant CD87 or Plg. Bound material was then analyzed using the H902 mAb. The full-length receptor (Δ0) as well as the mutants lacking domains 2–5 (Δ2–5), 6–9 (Δ6–9), 2–9 (Δ2–9), or 9–14 (Δ9–14) and the smallest form containing only the N-terminal part (Δ0.5–15) were all able to bind to Plg and CD87. In contrast, the truncated form lacking the N-terminal region (Δ0.5) did not exhibit binding of either Plg or CD87 (Fig. 6*A* and data not shown). The binding of both Δ0 and Δ0.5–15 to Plg was lysine-dependent because it was abolished in the presence of TA (Fig. 6*B*). Thus, the N-terminal part of CD222 appeared to be crucial for binding of both Plg and CD87.

The N-terminal Region of CD222 Is Similar to the Plg-binding Region in Streptokinase, and a Peptide Derived from That Region Can Disrupt the CD222-CD87 Complex—Comparison of the amino acid sequence of the N terminus of CD222 with already characterized Plg-binding proteins revealed similarity with the N-terminal part of streptokinase (Fig. 7). Streptokinase is a protein secreted by streptococci with the potential to degrade tissue barriers by binding and activating Plg (35). The region of streptokinase similar to the N terminus of CD222 was shown to share a common epitope with the putative Plg-binding site of fibronectin (36).

The sequences were compared by using ClustalW multiple alignment at the Network Protein Sequence @nalysis web server (npsa-pbil.ibcp.fr/cgi-bin/npsa_automat.pl?page=/NPSA/npsa_clustalw.html). This analysis revealed 20, 10, or 29% identical, as well as 32, 40, or 30% similar residues between the sequence stretches of CD222/streptokinase, CD222/fibronectin, or streptokinase/fibronectin, respectively (Fig. 7). Then we evaluated the significance of the protein sequence alignment by using the PRSS3 program at the Swiss node of EMBnet (www.ch.embnet.org/software/PRSS_form.html). PRSS3 repeatedly shuffles one of the sequences that are compared and calculates optimal similarity scores using the Smith-Waterman algorithm. We selected 1000 shuffles, window size 10, blosum50 scoring matrix, and gap opening/extension penalty 10/1. Using this setting, the similarity scores for the sequence stretches CD222/streptokinase, CD222/fibronectin, or streptokinase/fibronectin were 46, 29, or 76, respectively, corresponding to 4.9, 213, or 1.9 expectations for 1000 sequences. This means the likelihood to obtain by chance a similarity score of 46, as found for CD222 and streptokinase, is 4.9 in 1000 sequence comparisons. In contrast, with 213/1000 there is no similarity between CD222 and fibronectin.

This sequence relatedness between CD222 and streptokinase together with the results from the mapping analysis of CD222 prompted us to design peptides based on the N-terminal sequence of CD222 and to analyze their influence on CD222-CD87 interaction and function.

Two peptides were synthesized: pepB, derived from the stretch similar to the site in streptokinase playing a crucial role for Plg binding (37); and pepC, derived from the sequence corresponding to the site of streptokinase involved in Plg activation rather than binding (38) (Fig. 7). The peptides were contrived to encompass both the conserved residues and the lysines implicated in Plg binding. To avoid formation of cyclic or self-assembled peptides, which we had experienced in our previous studies with cysteine-containing peptides (data not shown), we replaced the cysteine in CD222 by alanine in the

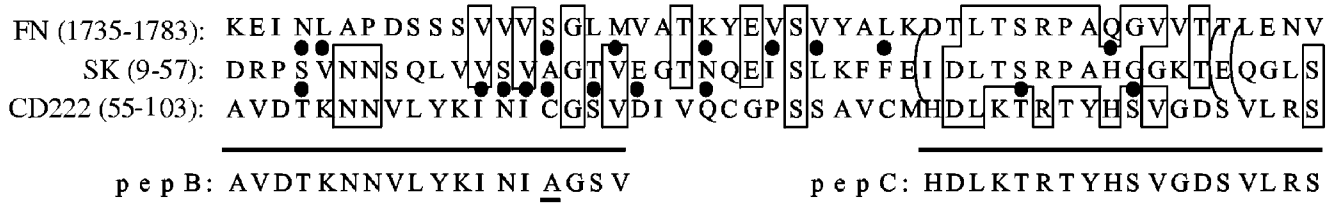

FIG. 7. **Alignment of the N-terminal region of CD222 (amino acids 55–103) with the Plg binding regions of streptokinase (*SK*, amino acids 9–57) and fibronectin (*FN*, amino acids 1735–1783).** Conserved residues are *framed*, and conservative exchanges are indicated by *dots* or *parentheses*, respectively. The peptides (pepB and pepC) derived from that region are shown. Alanine within the pepB sequence that replaced cysteine in CD222 is *underlined*. Amino acids of CD222 were counted including the 40-residue-long leader sequence.

pepB sequence (Fig. 7). As a control, we used a scrambled version of pepB, pepB*scr,* and pepA derived from domain 15 of CD222.

To test these peptides for their ability to influence the interaction of CD222 with CD87 in cells, $CD222^+/CD87^+$ cells and monocytes, in which the complex of CD222 with CD87 was originally described (26), were used. Cells were lysed, and the lysates were subjected to immunoprecipitation in the presence and absence of the peptides. PepB (but not pepC or the control peptides, pepB*scr* and pepA) was able to disturb the physical interaction of CD222 and CD87 (Fig. 8 and data not shown).

The Peptide Derived from the N-terminal Region of CD222 Can Modulate CD87-dependent Functions—Next, we examined the peptides described above for their ability to modulate the functions of CD87. In particular, we found that pepB abolished the uPA-induced induction of Plg activation, as well as adhesion to and chemotaxis on vitronectin through $CD87^+$ transductants (Fig. 9). It also inhibited the density-dependent responses of $CD222^+/CD87^+$ cells (data not shown). PAI-1 was used as a control inhibitor (Fig. 9*A*), and the results are in accord with published data (3, 39–41). PAI-1 reduced also the basal adhesion of the $CD87^+$ cells to vitronectin, which is the cause of the 120% inhibition. The median inhibitory concentration (IC_{50}) of pepB for uPA-induced adhesion of $CD87^+$ cells on vitronectin was found to be ~10 μM (Fig. 9*B*). The other peptides used in these experiments (pepB*scr*, pepC, pepA) had no or little effect.

Finally, we tested whether the peptides had any effect in cells expressing both CD87 and CD222 under normal conditions. Human monocytes fulfill this criterion and are additionally known to employ CD87 for cell migration (11). As shown in Fig. 10, pepB but not pepC or control peptides, pepB*scr* and pepA, reduced Plg activation by 34 ± 2%. Furthermore, when human PBMCs were allowed to adhere to vitronectin, uPA-induced cell adhesion was suppressed by 59 ± 6% in the presence of pepB, and the chemotactic response to uPA was reduced by 53 ± 8%. For comparison and as a control, PAI-1 known to inhibit uPA-mediated functions (3, 39–41) was included. Furthermore, we found that pepB was able to inhibit by 80% the uPA-induced migration of human smooth muscle cells, another cell type that migrates in response to uPA (42). These data are in good agreement with those obtained with the transduced mouse fibroblasts. In summary, we show that a peptide (pepB) derived from the N terminus of CD222 mimics the effect of CD222 on CD87-mediated Plg activation, cell adhesion, and chemotaxis.

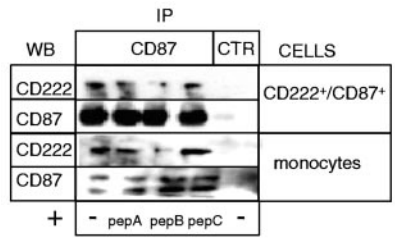

FIG. 8. **Effect of the CD222-derived peptides on the interaction of CD222 with CD87.** Immunoprecipitation analysis of $CD222^+/CD87^+$ cells and monocytes was performed in the presence of 20 μM amounts of the indicated peptides. Immunoprecipitates (*IP*) obtained with CD87 mAb H2 or IgG control mAb (*CTR-H902*) were analyzed by Western blotting (*WB*) using either the mAb mixture against CD222 (mix of mAbs MEM-238 and MEM-240) or CD87 mAb C8. One representative of five independent experiments is shown.

DISCUSSION

In the present study we provide for the first time evidence that CD222, which directly binds CD87 and Plg (25, 26), is a regulator of fibrinolysis and cell migration. By gene transfer we were able to show that CD222 expression down-regulated CD87-mediated Plg activation, cell adhesion, and chemotaxis. Furthermore, a peptide derived from the region within CD222 could be identified as critical for the interaction with CD87 and Plg, and was effective in modulation of CD87-mediated functions.

Mouse CD222-negative fibroblasts expressing human CD87 displayed augmented cell surface-associated Plg activation. This finding is in agreement with the established model that binding of uPA to CD87 leads to amplification of cell surface-associated proteolytic activity. PAI-1, a potent inhibitor of uPA, inhibited activation of Plg, confirming the Plg activator dependence of this process. The activation was also totally abolished in the presence of TA, a lysine analogue known to prevent Plg binding to lysine-binding sites on cells (43, 44), indicating that binding of Plg to cells was required for its activation. Co-expression of human CD222 reduced the enhanced ability of $CD87^+$ cells to activate Plg. This finding was the first to indicate that CD222 had a regulatory effect on CD87-mediated functions.

In addition to its contribution to the proteolytic cascade, CD87 participates also in cell adhesion and chemotaxis. Occupancy of CD87 by uPA promoted cell adhesion to vitronectin, an abundant component of the extracellular matrix (8, 9), and chemotactic locomotion of different cell types was induced by uPA binding to CD87 (10–13). Our model system is consistent with and confirms these findings. Expression of human CD87 in mouse CD222−/− fibroblasts caused significantly enhanced adhesion to vitronectin, and this increase was more profound in the presence of uPA (Fig. 3). Furthermore, the uPA-induced chemotactic locomotion of $CD87^+$ fibroblasts was significantly higher as compared with the untransduced parental cells. PAI-1 inhibited both the uPA-induced cell adhesion and chemotaxis of $CD87^+$ cells. This inhibition is in accord with previous studies demonstrating down-regulation of adhesion and chemotaxis by PAI-1 through either inhibition of CD87 binding to vitronectin (45) and/or promotion of CD87 internalization by CD91 (41) and, thus, confirms the uPA/CD87 dependence of these processes in these cells. Noteworthy, as in the Plg activation assay, expression of CD222 reversed the uPA/CD87-

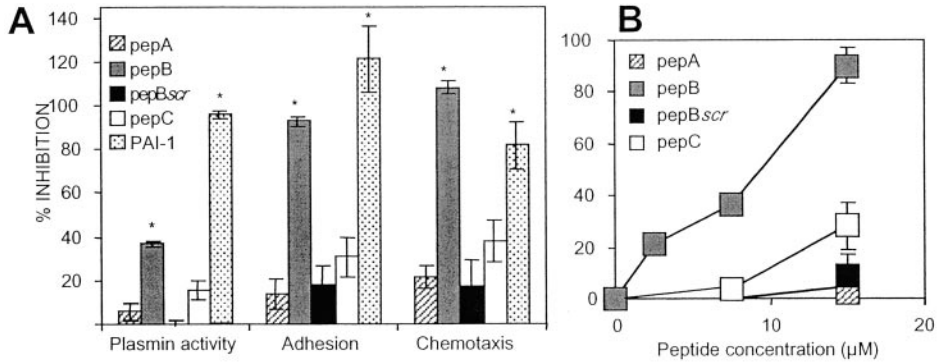

FIG. 9. **Effects of the CD222-derived peptides on uPA-induces functions with CD87$^+$ fibroblast transductants.** *A*, the Plg activation assay, the adhesion assay on vitronectin, and the chemotaxis assay were performed as described in Fig. 2, 3, or 4, respectively, in the presence of either 15 μM amounts of the indicated peptides or 10 units/ml PAI-1. The inhibition of 0% corresponds to the value obtained in the presence of uPA alone; the inhibition of 100% corresponds to the value obtained in the absence of uPA. *B*, IC_{50} determination of the effect of the peptides on cell adhesion to vitronectin. Basically, the cell adhesion assay was performed as described in Fig. 3*B* in the presence of 10 nM uPA alone or together with increasing peptide concentration plotted on the *x* axis (μM). Experiments were repeated three times in duplicate; the mean values ± S.D. (*, $p < 0.05$) are shown.

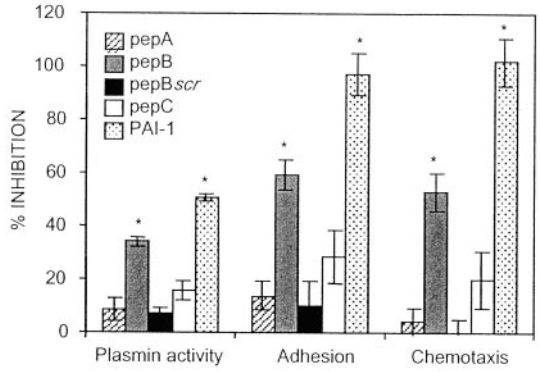

FIG. 10. **Effects of the CD222-derived peptides on uPA-induced functions with human monocytes and PBMCs.** The Plg activation assay was performed with monocytes adhered to a 96-well plate as described with fibroblasts (Fig. 2) in the presence of 15 μM peptides or 10 units/ml PAI-1. Plasmin activity was measured after 6 h. The cell adhesion assay was carried out with human PBMCs. The assay was performed as with fibroblasts (Fig. 3) in the presence of 10 nM uPA alone or together with 15 μM peptides or 10 units/ml PAI-1. The chemotaxis assay was performed with PBMCs as in Fig. 4 in the presence of 10 nM uPA alone or together with 15 μM peptides or 10 units/ml PAI-1. The inhibition of 0% corresponds to the value obtained in the presence of uPA alone; the inhibition of 100% corresponds to the value obtained in the absence of uPA. Experiments were repeated three times in duplicate; the mean values ± S.D. (*, $p < 0.05$) are shown.

mediated adhesion and chemotaxis.

To understand how CD222 affects CD87 functions at the molecular level, we mapped the binding sites for CD87 and Plg on CD222. Our data demonstrate that the N-terminal region of CD222 is critical for binding of both CD87 and Plg. The relevance of the N-terminal region of CD222 in this interaction is underlined by its similarity to the N-terminal part of streptokinase (Fig. 7), which binds and activates Plg, thereby facilitating invasion of bacteria through the host tissue barriers. The stretch around Val^{19} in the N terminus of streptokinase is implicated in Plg binding (35, 37), and that around Leu^{42} is involved in activation of Plg (38). From the corresponding sequences within the N terminus of CD222, we designed two peptides, termed pepB and pepC, respectively. PepB but not pepC was able to disrupt physical interaction of CD222 with CD87 as shown by co-precipitation analysis. Moreover, the same peptide had an inhibitory effect on uPA/CD87-mediated Plg activation, cell adhesion, and chemotaxis of CD87$^+$ single transductants, the density-dependent responses of CD222$^+$/CD87$^+$ transductants, as well as the responses of monocytes. Therefore, it is tempting to speculate that we have established an agonistic peptide from CD222, which targets CD222-free forms of CD87 and thereby mimics the inhibitory effect of endogenous CD222 on CD87.

Several possibilities can be envisaged of how CD222 controls CD87 functions. First, steric hindrance could lead to masking of uPA binding sites on CD87 by CD222 and thus to the blockade of CD87 functions. Second, the finding of Nykjaer and colleagues (25) showing that CD222 targets CD87 into lysosomes suggests internalization of CD87 by CD222 followed by degradation of CD87. This pathway might be different from the CD91-mediated internalization, ligand clearing, and recycling of CD87, which leads to re-activation instead of termination of CD87 functions (18, 19). Third, interaction of CD222 with CD87 could influence the ligand binding capacity of CD87 by changing the CD87 conformation. Finally, binding of CD222 and CD87 could alter the complex formation of CD87 with other membrane partners, Src kinases (46), integrins (14), CD91 (18), CD130 (47), caveolin (48), L-selectin (49), and thereby the functions underlying these molecular interactions.

The platforms of these interactions seem to be GPI microdomains or lipid rafts (14, 26, 48, 50). These plasma membrane compartments are more and more viewed as to control receptor signaling across the plasma membrane and execution of receptor functions at the membrane by facilitating association/dissociation of receptors, transmembrane adaptors, and submembrane signaling components (51). These microdomains are characterized by low density and by the enrichment of the GPI proteins expressed in a given cell, glycosphingolipids, cholesterol, and Src kinases; they are also devoid of most transmembrane receptor proteins. The "CD87 microdomain" of monocytes is special, as it harbors among GPI proteins exclusively CD87 and contains as constitutive components the transmembrane receptors CD222 and integrins (14, 26). Human CD87 and human CD222 meet also in the membrane of the mouse fibroblast transductants in such low density microdomains (Fig. 1 and data not shown).

CD222 circles between trans-Golgi network, lysosomes, plasma membrane, and endosomes with a rapid turnover. This trafficking appears to be regulated by a variety of factors including CD222 ligands, growth factors, retinoic acid, and phorbol esters (52–55). Thus, the number of CD222 molecules in the plasma membrane can be rapidly changed in response to various stimuli. In respect to our data, this shuttling might allow cells a tight and quick control of cell surface-associated proteolysis, adhesion, and chemotaxis. CD222 was proposed as a

tumor suppressor by, *e.g.*, scavenging of the growth factor IGF2, activation of transforming growth factor-β1 (56). The loss of CD222 function may, therefore, not only lead to uncontrolled growth but also to loss of control over CD87 and consequently to elevated pericellular proteolysis and increased invasion of tumor cells.

Acknowledgments—We thank Dr. E. Wagner and Dr. G. P. Nolan for providing CD222−/− mouse fibroblasts and the Phoenix packaging cell line, respectively. We are grateful to Andreas Szekeres, Günther Staffler, Karel Drbal, and Sawitree Chiampanichayakul for plasmid constructs, cells, and helpful discussions. We acknowledge Petra Haderer, Sabine Swoboda, and Eva Steinhuber for excellent technical assistance.

REFERENCES

1. Dunon, D., Piali, L., and Imhof, B. A. (1996) *Curr. Opin. Cell Biol.* **8,** 714–723
2. Sendo, F., and Araki, Y. (1999) *J. Leukocyte Biol.* **66,** 369–374
3. Blasi, F. (1997) *Immunol. Today* **18,** 415–417
4. Behrendt, N., Rønne, E., and Danø, K. (1995) *Biol. Chem. Hoppe Seyler* **376,** 269–279
5. Plow, E. F., Herren, T., Redlitz, A., Miles, L. A., and Hoover-Plow, J. L. (1995) *FASEB J.* **9,** 939–945
6. Waltz, D. A., Fujita, R. M., Yang, X., Natkin, L., Zhuo, S., Gerard, C. J., Rosenberg, S., and Chapman, H. A. (2000) *Am. J. Respir. Cell Mol. Biol.* **22,** 316–322
7. van der Pluijm, G., Sijmons, B., Vloedgraven, H., van der Bent C., Drijfhout, J. W., Verheijen, J., Quax, P., Karperien, M., Papapoulos, S., and Lowik, C. (2001) *Am. J. Pathol.* **159,** 971–982
8. Waltz, D. A., and Chapman, H. A. (1994) *J. Biol. Chem.* **269,** 14746–14750
9. Wei, Y., Waltz, D. A., Rao, N., Drummond, R. J., Rosenberg, S., and Chapman, H. A. (1994) *J. Biol. Chem.* **269,** 32380–32388
10. Boyle, M. D., Chiodo, V. A., Lawman, M. J., Gee, A. P., and Young, M. (1987) *J. Immunol.* **139,** 169–174
11. Gyetko, M. R., Todd, R. F., III, Wilkinson, C. C., and Sitrin, R. G. (1994) *J. Clin. Invest.* **93,** 1380–1387
12. Resnati, M., Guttinger, M., Valcamonica, S., Sidenius, N., Blasi, F., and Fazioli, F. (1996) *EMBO J.* **15,** 1572–1582
13. Fazioli, F., Resnati, M., Sidenius, N., Higashimoto, Y., Appella, E., and Blasi, F. (1997) *EMBO J.* **16,** 7279–7286
14. Bohuslav, J., Horejsi, V., Hansmann, C., Stockl, J., Weidle, U. H., Majdic, O., Bartke, I., Knapp, W., and Stockinger, H. (1995) *J. Exp. Med.* **181,** 1381–1390
15. Wei, Y., Lukashev, M., Simon, D. I., Bodary, S. C., Rosenberg, S., Doyle, M. V., and Chapman, H. A. (1996) *Science* **273,** 1551–1555
16. Xue, W., Mizukami, I., Todd, R. F., III, and Petty, H. R. (1997) *Cancer Res.* **57,** 1682–1689
17. Wei, Y., Yang, X., Liu, Q., Wilkins, J. A., and Chapman, H. A. (1999) *J. Cell Biol.* **144,** 1285–1294
18. Conese, M., Nykjaer, A., Petersen, C. M., Cremona, O., Pardi, R., Andreasen, P. A., Gliemann, J., Christensen, E. I., and Blasi, F. (1995) *J. Cell Biol.* **131,** 1609–1622
19. Zhang, J. C., Sakthivel, R., Kniss, D., Graham, C. H., Strickland, D. K., and McCrae, K. R. (1998) *J. Biol. Chem.* **273,** 32273–32280
20. Vilhardt, F., Nielsen, M., Sandvig, K., and van Deurs, B. (1999) *Mol. Biol. Cell* **10,** 179–195
21. Godár, S., Leksa, V., Cebecauer, M., Hilgert, I., Horejsi, V., and Stockinger, H. (2002) in *Leukocyte Typing VII* (Mason, D., Andre, P., Bensussan, A., Buckley, C., Civin, C., Clark, E., de Haas, M., Goyert, S., Hadam, M., Hart, D., Horejsi, V., Jones, Y., Meuer, S., Morrissey, J., Schwarz-Albiez, R., Shaw, S., Simmons, D., Turni, L., Uguccioni, M., van der Schoot, E., Vivier, E., and Zola, H., eds) pp. 482–485, Oxford University Press, Oxford
22. Kornfeld, S. (1992) *Annu. Rev. Biochem.* **61,** 307–330
23. Dahms, N. M. (1996) *Biochem. Soc. Trans.* **24,** 136–141
24. Godár, S., Leksa, V., Horejsi, V., and Stockinger, H. (2000) in *Protein Reviews on the Web (http://www.ncbi.nlm.nih.gov/prow/guide/233853413_g.htm)* (Shaw, S., Turni, L. A., and Katz, K. S., eds) Vol. 1, pp. 50–55
25. Nykjaer, A., Christensen, E. I., Vorum, H., Hager, H., Petersen, C. M., Roigaard, H., Min, H. Y., Vilhardt, F., Moller, L. B., Kornfeld, S., and Gliemann, J. (1998) *J. Cell Biol.* **141,** 815–828
26. Godár, S., Horejsi, V., Weidle, U. H., Binder, B. R., Hansmann, C., and Stockinger, H. (1999) *Eur. J. Immunol.* **29,** 1004–1013
27. Rønne, E., Behrendt, N., Ploug, M., Nielsen, H. J., Wollisch, E., Weidle, U., Danø, K., and Hoyer-Hansen, G. (1994) *J. Immunol. Methods* **167,** 91–101
28. Wang, Z. Q., Fung, M. R., Barlow, D. P., and Wagner, E. F. (1994) *Nature* **372,** 464–467
29. Swift, S., Lorens, J., Achacoso, P., and Nolan, G. P. (1999) in *Current Protocols in Immunology,* (Coligan, J. E., Kruisbeek, A. M., Margulies, D. H., Shevach, E. M., and Strober, W., eds) pp. 10.17.14–10.17.29, Green Publishing Associates and Wiley-Interscience, New York
30. Kinoshita, S., Su, L., Amano, M., Timmerman, L. A., Kaneshima, H., and Nolan, G. P. (1997) *Immunity* **6,** 235–244
31. Pear, W. S., Nolan, G. P., Scott, M. L., and Baltimore, D. (1993) *Proc. Natl. Acad. Sci. U. S. A.* **90,** 8392–8396
32. Ellis, V., Behrendt, N., and Danø, K. (1993) *Methods Enzymol.* **223,** 223–233
33. Scott, C. D., Taylor, J. E., and Baxter, R. C. (1988) *Biochem. Biophys. Res. Commun.* **151,** 815–821
34. Baier, G., Baier Bitterlich, G., Couture, C., Telford, D., Giampa, L., and Altman, A. (1994) *BioTechniques* **17,** 94–99
35. Wang, X., Lin, X., Loy, J. A., Tang, J., and Zhang, X. C. (1998) *Science* **281,** 1662–1665
36. Gonzalez-Gronow, M., Enghild, J. J., and Pizzo, S. V. (1993) *Biochim. Biophys. Acta* **1180,** 283–288
37. Kim, D. M., Lee, S. J., Kim, I. C., Kim, S. T., and Byun, S. M. (2000) *Thromb. Res.* **99,** 93–98
38. Liu, L., Sazonova, I. Y., Turner, R. B., Chowdhry, S. A., Tsai, J., Houng, A. K., and Reed, G. L. (2000) *J. Biol. Chem.* **275,** 37686–37691
39. Kanse, S. M., Kost, C., Wilhelm, O. G., Andreasen, P. A., and Preissner, K. T. (1996) *Exp. Cell Res.* **224,** 344–353
40. Deng, G., Curriden, S. A., Wang, S., Rosenberg, S., and Loskutoff, D. J. (1996) *J. Cell Biol.* **134,** 1563–1571
41. Degryse, B., Sier, C. F., Resnati, M., Conese, M., and Blasi, F. (2001) *FEBS Lett.* **505,** 249–254
42. Kusch, A., Tkachuk, S., Lutter, S., Haller, H., Dietz, R., Lipp, M., and Dumler, I. (2002) *Biol. Chem.* **383,** 217–221
43. Lee, S. W., Ellis, V., and Dichek, D. A. (1994) *J. Biol. Chem.* **269,** 2411–2418
44. Ellis, V., Whawell, S. A., Werner, F., and Deadman, J. J. (1999) *Biochemistry* **38,** 651–659
45. Waltz, D. A., Natkin, L. R., Fujita, R. M., Wei, Y., and Chapman, H. A. (1997) *J. Clin. Invest.* **100,** 58–67
46. Stefanova, I., Horejsi, V., Ansotegui, I. J., Knapp, W., and Stockinger, H. (1991) *Science* **254,** 1016–1019
47. Koshelnick, Y., Ehart, M., Hufnagl, P., Heinrich, P. C., and Binder, B. R. (1997) *J. Biol. Chem.* **272,** 28563–28567
48. Chapman, H. A., Wei, Y., Simon, D. I., and Waltz, D. A. (1999) *Thromb. Haemostasis* **82,** 291–297
49. Sitrin, R. G., Pan, P. M., Blackwood, R. A., Huang, J., and Petty, H. R. (2001) *J. Immunol.* **166,** 4822–4825
50. Koshelnick, Y., Ehart, M., Stockinger, H., and Binder, B. R. (1999) *Thromb. Haemostasis* **82,** 305–311
51. Horejsi, V., Cebecauer, M., Cerny, J., Brdicka, T., Angelisova, P., Drbal, K., and Stockinger, H. (1999) *Immunol. Today* **20,** 356–361
52. Braulke, T., Tippmer, S., Neher, E., and von Figura, K. (1989) *EMBO J.* **8,** 681–686
53. Prence, E. M., Dong, J. M., and Sahagian, G. G. (1990) *J. Cell Biol.* **110,** 319–326
54. Zhang, Q., Berggren, P. O., and Tally, M. (1997) *J. Biol. Chem.* **272,** 23703–23706
55. Kang, J. X., Bell, J., Leaf, A., Beard, R. L., and Chandraratna, R. A. (1998) *Proc. Natl. Acad. Sci. U. S. A.* **95,** 13687–13691
56. De Souza, A. T., Yamada, T., Mills, J. J., and Jirtle, R. L. (1997) *FASEB J.* **11,** 60–67